Chinese Journal of Polymer Science Vol. 35, No. 8, (2017), 1009–1019

Chinese Journal of Polymer Science

The Effect of Self-nucleation on Isothermal Crystallization Kinetics of Poly(butylene succinate) (PBS) Investigated by Differential Fast Scanning Calorimetry*

Jing Jiang[a], Evgeny Zhuravlev[a, c], Wen-bing Hu[a], Christoph Schick[c] and Dong-shan Zhou[a, b**]
[a] *Department of Polymer Science and Engineering, School of Chemistry and Chemical Engineering, State Key Laboratory of Coordination Chemistry, Nanjing University, Nanjing 210023, China*
[b] *School of Physical Science and Technology, Xinjiang Key Laboratory and Phase Transitions and Microstructures in Condensed Matters, Yili Normal University, Yining 835000, China*
[c] *University of Rostock, Institute of Physics, Wismarsche Strasse 43-45, 18051 Rostock, Germany*

Abstract Differential fast scanning calorimetry (DFSC) was employed on the study of self-nucleation behavior of poly(butylene succinate) (PBS). The ultra-fast cooling ability of DFSC allows investigating the effect of self-nucleation on the isothermal crystallization kinetics over a wide temperature range. Crystallization half-time, instead of crystallization peak temperature, was used to describe the self-nucleation behavior, and the self-nucleation domain for the samples crystallized at different temperatures was determined. Due to the competition between homogenous nucleation and self-nuclei, the effect of self-nucleation was less pronounced at high supercooling than that for the sample isothermally crystallized at higher temperature. An efficiency scale to judge the efficiency of nucleating agents from the crystallization half-time was also introduced in this work.

Keywords Self-nucleation; Differential scanning calorimetry; Fast scanning calorimetry; Nucleation efficiency; Poly(butylene succinate)

INTRODUCTION

Self-nucleation (or self-seeding) is a unique phenomenon for semi-crystalline polymers which show a large melting temperature range. It allows co-existence of molten and crystalline regions at a given temperature in a same sample[1]. Numerous early studies reported that the seeds obtained from the fragmentation of partially molten crystals could effectively lower the free energy barrier for the nucleation and increase the overall crystallization rate[2–10]. With self-seeding, the crystallization temperature of the sample could be 25 K higher than that from the equilibrated random coil, and the number of nuclei could be increased by several orders of magnitude. Since most commercial crystalline polymers are processed from the melt, self-nucleation can shorten molding or solidification cycles and improve optical properties by reducing the size of the spherulites due to enhanced nucleation density. It is of significance to study the self-nucleation (SN) behavior of polymers either for scientific research or for practical application. A seminal work was presented by Fillon *et al.*[2], adapting self-nucleation procedures to differential scanning calorimetry (DSC). Their detailed investigations on isotactic

* This work was financially supported by the National Natural Science Foundation of China (Nos. 21474049, 51673094 and 21404055), the Shenzhen Science and Technology Innovation Committee (Nos. JCYJ20160531151102203 and JCYJ20160608140827794), and Tianshan Scholars Program by Yili Normal University.
** Corresponding author: Dong-shan Zhou (周东山), E-mail: dzhou@nju.edu.cn
Received December 30, 2016; Revised January 23, 2017; Accepted February 8, 2017
doi: 10.1007/s10118-017-1942-5

polypropylene enabled the division of the melting temperature range into three domains. Domain I is defined as the high temperature range where complete melting occurs and no self-nucleation or annealing takes place. In domain II or SN domain, almost all of the polymer crystals melt but leave some small crystal self-nuclei or seeds, resulting in an exponential increase in nucleation density. Correspondingly, it is observed that the crystallization temperature (T_c) shifts to higher values upon cooling from lower self-nucleation temperature (T_s). In domain III, T_s is low enough to leave some unmelt crystal lamellae, resulting in annealing and thickening of the original lamellae.

Over the past decades, various characterization techniques, such as differential scanning calorimetry, optical microscopy and rheological measurements, have been applied to study self-nucleation in polymers. The self-nucleation behavior of various polymers (including copolymers) has been investigated. The effects of annealing time and different molecular weights on self-nucleation behavior were studied[8, 9, 11–16]. Compared to homopolymers, the crystallization of random copolymers that contained a unique sequence selection and a strong memory effect of their prior crystallization could be observed even at temperature above the equilibrium melting point[17, 18]. This memory effect might be attributed to the seeds made of segregated segments without any crystalline nature which could also accelerate the subsequent crystallization. The polymorphic change of random copolymers in subsequent crystallization depending on the initial polymorph or melt temperature was also studied recently, which offered help to discuss the mechanism of polymorph selection of copolymers during crystallization[18–20]. A so-called 'efficiency scale' for nucleation additives of polymers is also established from self-nucleation experiments performed with conventional DSC[3]. Judging the nucleation efficiency is commonly done by comparing the crystallization peak temperature on cooling from the melt in DSC at a cooling rate of 10 K/min as proposed by Fillon *et al*[21]. However, because of the limited cooling abilities of conventional DSC, a saturation of the nucleating effect can be found as a small number of active nuclei at high crystallization temperatures are sufficient to allow the sample to fully crystallize within the time defined by the slow DSC experiment[22, 23]. Isothermal crystallization experiments of samples performed on DSC are also limited to a high temperature range due to the slow cooling. Recently, Zhuravlev *et al*. employed a new powerful tool, differential fast scanning calorimetry (DFSC), to investigate the efficiency of nucleating agents on polymers. The ultra-fast cooling ability of DFSC allows to judge the nucleation efficiency in the whole range of temperatures where the semi-crystalline polymers crystalize[13, 23].

Differential fast scanning calorimetry (DFSC) is a sensitive characterization technique to get insight into structure formation in fast crystallizing polymers. It gives unique possibility for an insight on polymer crystal nucleation and growth[24–27]. The isothermal crystallization measurement (*e.g.* crystallization half-time) was found to be a sensitive tool to investigate the crystal nucleation, reorganization and disordering in the sample. Different levels of ordering obtained from the cooling process will affect the experimental results in the final stage of heating, thus a reheating method can be used to study the kinetics of nucleation under isothermal conditions as described in the previous reports[28, 23]. Using multi-step annealing experiments allows to gain deeper insight into crystal nuclei formation at large undercooling[29]. An advantage of DFSC compared to conventional DSC is the fast scanning rates up to 10^6 K/s, which can prevent reorganization, *i.e.* nucleation and growth, during both fast heating and cooling, thus allowing to study *e.g.* isothermal crystallization of the samples after thermal conditioning at selected T_s. Among recent works, Martino *et al*. applied fast scanning calorimetry to investigate the self-nucleation of poly(ethylene 2,5-furandicarboxylate) (PEF). The SN domain in their work was described by the change of melting behavior of a sample nucleated under different thermal treatments and crystallized under fixed isothermal conditions in analogy to previous conventional DSC studies[30]. In the present work, we use the half-time of crystallization to characterize the self-nucleation. In addition, we also use the crystallization half-time to calculate the efficiency of nucleating agents at different crystallization temperatures, which is of high interest for industrial processing.

In this paper, a systematic investigation on the self-nucleation behavior of pure poly(butylene succinate) (PBS) was carried out using conventional DSC and DFSC, employing the conventional SN procedure developed by Fillon *et al*[2]. Polarized optical microscopy (POM) was also applied to observe the crystalline morphologies

of the crystallized samples after different thermal conditioning. A modified SN procedure was used in DFSC measurements to study the self-nucleation effect on the kinetics of isothermal crystallization of PBS. The change of crystallization half-time $\tau_{1/2}$, instead of crystallization temperature T_c, was used to describe the self-nucleation behavior as T_s changed. The nucleating efficiency scale for PBS samples was calculated from T_c and $\tau_{1/2}$ too. A PBS sample blended with 2 wt% of poly(butylene fumarate) (PBF) was taken as an example to calculate the efficiency of nucleating agents from crystallization half-time.

EXPERIMENTAL

Materials

Poly(butylene succinate) (PBS) sample and PBS sample with 2 wt% of poly(butylene fumarate) (PBF) were provided by Prof. Jun Xu's group and used without further purification[31], and the detailed sample preparation was described in their previous work[31, 32]. The number-average molecular weight (M_n) and polydispersity (PDI) of PBS are 4.46×10^4 g/mol and 1.47, respectively.

Differential Scanning Calorimetry (DSC)

All the DSC experiments were performed in Mettler-Toledo DSC 1 with the heating and cooling rates at 10 K/min. Samples were encased in aluminum pans and an empty aluminum pan was used as a reference. The weights of the DSC samples were around 4 mg. Dry nitrogen gas flow (50 mL/min) was used for purging.

DSC thermal treatment protocol was same as the former reports[2, 3], which was composed of four steps (Fig. 1a): (1) heating the initial PBS samples at a rate of 10 K/min to 423 K and keeping for 5 min to erase the previous history, then creating the "standard" sample by cooling down to 298 K at a rate of 10 K/min; (2) heating the "standard" sample to self-nucleation temperature T_s and melting for 5 min; (3) recrystallizing the samples on cooling from T_s to 295 K at a rate of 10 K/min; (4) heating the resultant samples to 423 K, and recording the re-melting curves.

Differential Fast Scanning Calorimetry (DFSC)

Isothermal crystallization of PBS samples were studied by an ultra-fast scanning calorimeter. The details of instrument and sample preparation could be found in the previous reports[33, 34]. Figure 1(b) shows the thermal treatment protocol of DFSC for studying the effect of self-nucleation on the subsequent isothermal crystallization process. Similar to the protocol in DSC, there are four steps, including (1) crystallizing the samples at 320 K for 10 s as the history to generate a relatively stable initial state (the fast cooling process produced full amorphous samples, which needed isothermally crystalizing at a selected temperature to create a "standard" state); (2) heating up to self-nucleation temperature T_s for 0.001 s to achieve partial melting; (3) cooling at 1×10^4 K/s to a selected crystallization temperature T_{an} (320 or 260 K) and annealing for different time; (4) heating the samples to 420 K to investigate the melting peaks.

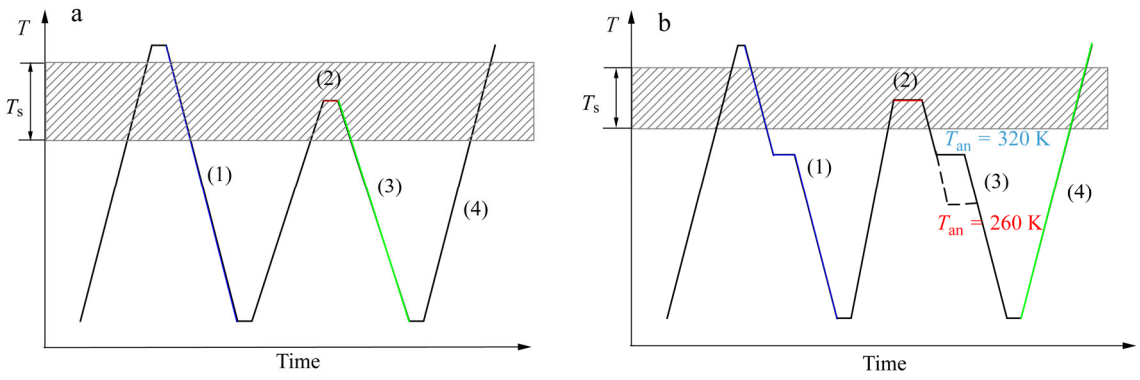

Fig. 1 Schemes for thermal treatment protocols in (a) DSC and (b) DFSC (Both are composed of 4 steps.)

Polarized Optical Microscopy (POM)

The crystalline morphology was investigated by a polarized optical microscope (Olympus DX14) with crossed polarizers. Thin melt samples were prepared between microscope cover slips, which were melted at 423 K for 5 min and then cooled down to room temperature at 10 K/min to obtain the standard morphology. Then, the samples were heated to different self-nucleation temperature T_s and cooled down to reproduce the conditions employed in DSC as described previously. The final crystalline morphology was obtained for each T_s.

RESULTS AND DISCUSSION

Self-nucleation Behavior in Conventional DSC

Figures 2 and 3 present the self-nucleation behavior of PBS observed with DSC. Figure 2(a) shows the cooling curves after thermal conditioning at the indicated T_s temperatures, and Fig. 3 exhibits the subsequent heating runs. After 5 min thermal treatments at selected T_s, the "standard" samples were partially melted to different extents and various crystallization peaks appeared in the subsequent cooling at a fixed cooling rate of 10 K/min. As shown in Fig. 2(a), decrease of T_s results in a significant increase of crystallization temperature T_c, indicating that more surviving "nuclei" are left in the polymer melt which increase the density of nucleation sites and accelerate the crystallization kinetics. The self-nucleation phenomenon proceeds until T_s reaches 388 K, where the concentration of remained crystalline fragments is high enough and the unmelted crystal starts to anneal (domain III). An additional high temperature melting peak marked with an arrow shows up on the subsequent second melting (step 4) as shown in Fig. 3 (T_s = 387 K). When T_s is above 405 K, samples are completely melted

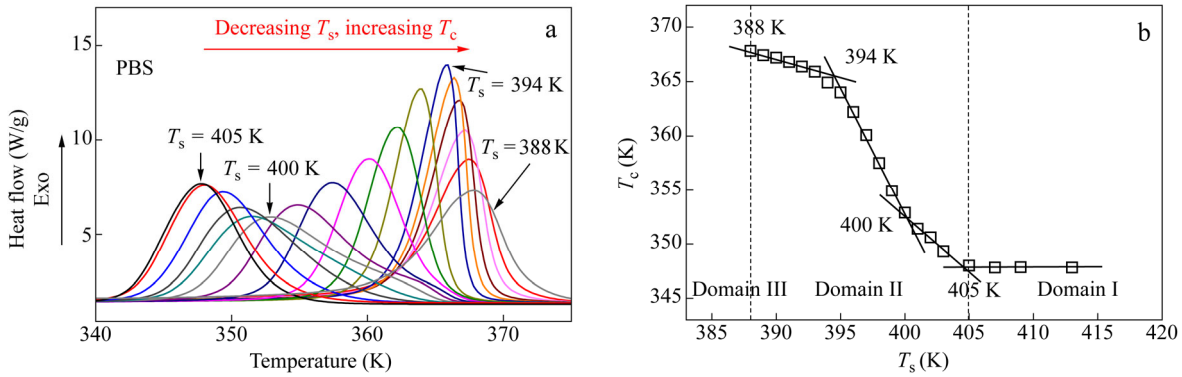

Fig. 2 (a) DSC cooling curves (at 10 K/min) after 5 min annealing at the indicated T_s (from 387 K to 407 K) (Decreasing T_s results in an increase of crystallization peak temperature T_c on the subsequent cooling.); (b) Variation of the peak crystallization temperature T_c as a function of self-nucleation temperature T_s

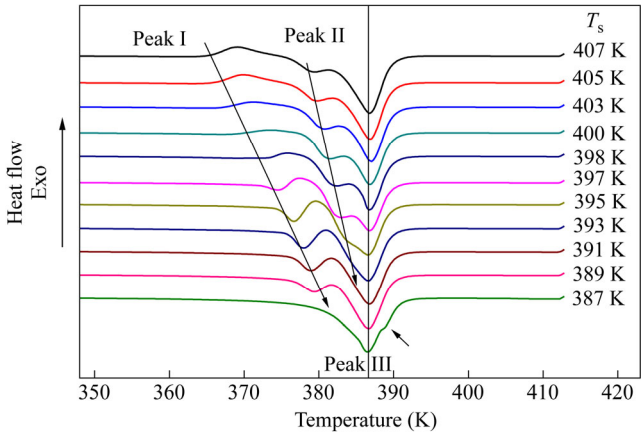

Fig. 3 Subsequent DSC heating curves (at 10 K/min) after controlled cooling scans shown in Fig. 2(a)

(domain I) and subsequent cooling simply reproduces the standard state with a crystallization peak located at 348 K. For all the crystallization peaks, the heat of crystallization (ΔH_c) keeps almost constant at (76 ± 2) J/g, indicating a similar crystallinity of the sample with different T_s.

The crystallization temperature T_c of self-nucleated samples is shown in Fig. 2(b) as a function of self-nucleation temperature T_s. According to the definition of self-nucleation domain (or domain II) proposed by Fillon *et al*.[2], PBS sample used here has a wide SN domain over 17 K and the crystallization temperature of PBS is increased by 20 K with self-nucleation. Two tuning points can be observed in domain II, one at T_s = 394 K and another at T_s = 400 K, where the crystallization peaks with maximum or minimum peak height are observed in the subsequent cooling curves (Fig. 2a), respectively.

Multiple melting peaks are observed in the reheating curves of PBS after crystallization (Fig. 3). Three melting peaks can be distinguished, marked as "peak I, peak II and peak III" respectively. The shoulder peak appears in the heating curve when T_s = 387 K is an evidence of unmelted crystal remained in the sample and the trademark of domain III (*i.e.* annealing as opposed to self-nucleation)[2]. Peak III appears at about 387 K in each measurement and depends on neither T_c nor T_s. This is usually the melting peak of reorganized crystals. Peak I originates from the thermal history. When the sample is reheated, it will melt and recrystallize to another crystal with higher stability whose melting peak corresponds to peak II. As T_s decreases, the sample crystallizes at higher temperature producing more stable crystals and leads a shift of peak I to higher temperature in the reheating curves. When T_s is lower than 393 K, stable crystals form during cooling (peak I) and can reorganize directly to the most stable one (peak III) in the subsequent heating.

Morphology of Self-nucleated Samples

Crystalline morphology of PBS sample is significantly affected by self-nucleation, similar to many other semi-crystalline polymers[7, 8, 11, 35]. Figure 4 displays selected optical micrographs of the morphologies formed *via* self-nucleation at different temperatures, corresponding to the samples treated by DSC in Fig. 2. The standard sample (cooled from 423 K without self-nucleation at 10 K/min) presents well-developed spherulites with distinct boundaries as shown in the last picture in Fig. 4. When T_s decreases, reduction in spherulite size and increase of nucleation density can be observed. For 400 K < T_s < 405 K, the spherulites of PBS are very compact and preserve the well-developed morphology of the original large spherulite in "standard" sample with some obvious self-seeds in the center. When T_s < 400 K, progressive fading of the original morphology appears and the morphology of crystals become mainly fan-shaped, leaving some spherulitic patterns. As T_s decreases further to below 391 K, the exponential increase in nucleation density results in the spherulite diameter decreasing dramatically, and only granular crystals can be seen. The morphology of PBS sample blended with 2 wt% PBS is also investigated by POM, which is the same as that of neat PBS after self-nucleated at T_s below 391 K.

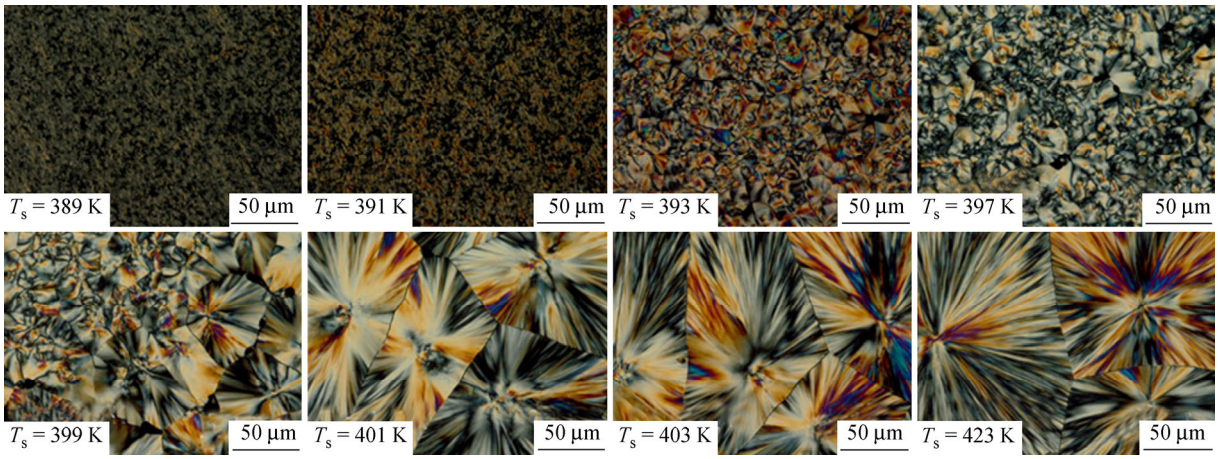

Fig. 4 POM micrographs of PBS after SN treatment at indicated T_s temperatures

Self-nucleation Behavior Investigated by DFSC

DFSC measurements were performed by following the thermal procedure showed in Fig. 1(b). A sample isothermally crystallized at 320 K for 10 s was used as the "standard" state, instead of the non-isothermally crystallized sample performed in conventional DSC. To study the effect of self-nucleation on the kinetics of isothermal crystallization, the crystallization half-time of PBS after self-nucleation at different T_s were compared with that of the original state. The kinetics of nucleation and crystallization in PBS nanocomposites has been studied by Papageorgiou *et al*[13]. According to their results, the nucleation mechanism of PBS changed at 280 K from heterogeneous to homogeneous. Two isothermal crystallization temperatures T_{an} were selected, 320 K and 260 K, which were close to the melting temperature or just above the end of glass transition of the samples, attributed to the heterogeneous or homogeneous nucleation dominating region respectively. A high cooling rate (1×10^4 K/s) was chosen to suppress additional crystallization or homogeneous nucleation on cooling. It is one of the main advantages of DFSC. After melted at different T_s for 0.001 s, the sample was cooled to selected T_{an} and annealed for different time t_{an}, expecting to realize different degrees of ordering. Then reheating curves were collected to investigate the different levels of ordering in the sample. This reheating method was already used in several previous reports to study the kinetics of nucleation in polymers under isothermal conditions[13, 23, 28, 36].

Reheating curves after isothermal crystallization experiments of PBS samples with or without SN are shown in Fig. 5. The results from the crystallization at 260 K show two separated melting peaks (Fig. 5b). The first one is attributed to the imperfect low temperature crystals, which melt just above the crystallization temperature and then reorganize even at 1×10^4 K/s heating rate to even more stable crystals melting at 350 K. However, the crystals formed at T_{an} = 320 K are more stable and the melting peaks integrate into one peak as the annealing time is long enough (Fig. 5a). The melting behaviors of self-nucleated samples are similar (Figs. 5c and 5d), but the crystallization time is dramatically shortened as T_s decreases. When T_s decreases further, an additional shoulder peak at higher temperature appears in the reheating curves (Figs. 5e and 5f), indicating that unmelted crystals remain and the thickening of original crystal lamellae occurs under the subsequent isothermal conditions, similar to that of conventional DSC.

The values of total latent heat (Δh) of the crystallized samples after annealing at T_{an} = 320 and 260 K with self-nucleation at selected T_s are shown in Figs. 6(a) and 6(c). A systematical shift to shorter crystallization time (indicating a speed up of crystallization rate) at each annealing temperature can be observed as T_s decreases, and the SN domain can be determined. The open square points (410 K) are attributed to the completely melted sample without self-nucleation. When T_s decreases, the curve starts to shift to shorter crystallization time at T_s = 390 K for T_{an} = 320 K, while for T_{an} = 260 K, it keeps unchanged until T_s = 380 K. As T_s decreases as low as possible, the nucleation induction plateau starts with a constant Δh (circled with red dotted line in Figs. 6a and 6c), instead of zero, indicating that unmelted crystals remain in the sample before isothermal crystallization, which can be seen as the trademark of domain III.

The results from the integration of experimental data were fitted according to the formalism proposed by Kolmogorov-Johnson-Mehl-Avrami (KJMA)[13, 23], and the obtained crystallization half-time ($\tau_{1/2}$) of PBS is plotted against self-nucleation temperature for each T_{an} in Figs. 6(b) and 6(d). For T_{an} = 320 K, PBS has a SN domain over 30 K from 360 K to 390 K, while for T_{an} = 260 K, the SN domain is narrower, about 15 K from 365 K to 380 K. As mentioned previously, isothermal crystallization at 260 K is dominated by homogeneous nucleation, and homogeneous nucleation may compete with the self-nuclei and overturn their influence. It can also be seen that the self-nucleation exhibits different levels of acceleration in isothermal crystallization of PBS. The high nucleated samples present two orders of magnitude faster crystallization in the region of heterogeneous nucleation (T_{an} = 320 K), while less than one order of magnitude is shown in the region of homogeneous nucleation (T_{an} = 260 K). Similar phenomena were reported for some polymer nanocomposites[13, 23].

Previously, the self-nucleation is commonly analyzed according to a methodology introduced by Fillon *et al*.[21], which rests on the analysis of impact of partial melting of the samples on subsequent crystallization as investigated in a DSC apparatus. The crystallization peak temperature on cooling is used to judge the nucleation efficiency of self-nuclei. A higher crystallization temperature is considered to indicate higher nuclei density in

the sample. However, the increase of crystallization peak temperature is an overall effect of nucleation and crystallization on cooling from the melt. Because of the limited cooling abilities of conventional DSC, a saturation of the nucleating effect can be found, as a small number of active nuclei at high crystallization temperatures are sufficient to allow the sample to fully crystallize within the time defined by the slow DSC experiment[22, 23]. In addition, the effect of self-nucleation on isothermal crystallization can only be studied in a very limited temperature range with conventional DSC, also due to its limited cooling ability. The samples have been crystallized on cooling before reaching lower temperatures.

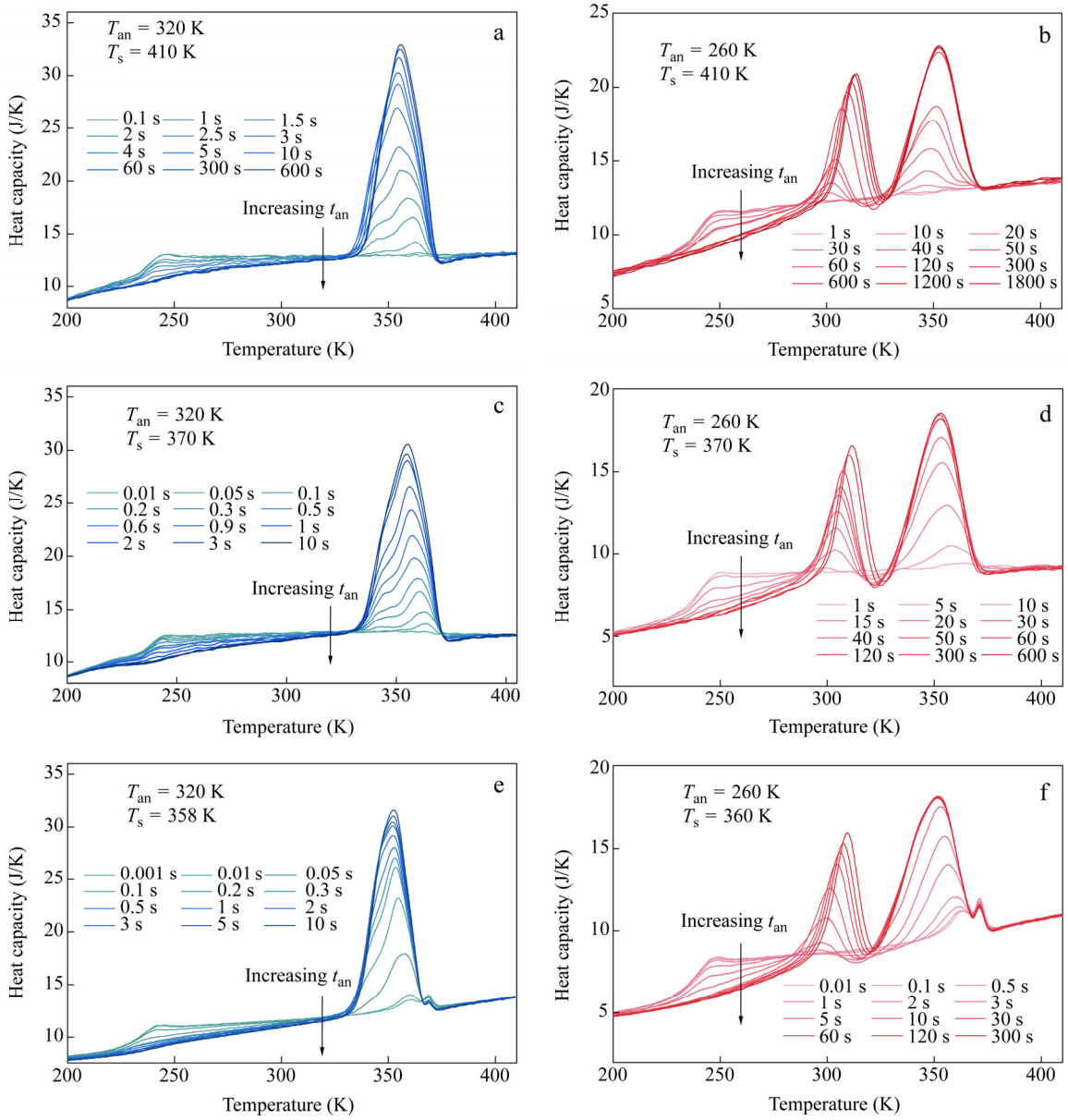

Fig. 5 Heat capacity of PBS isothermally crystallized samples from DFSC reheating curves annealing at (a, c, e) T_{an} = 320 K or (b, d, f) T_{an} = 260 K at a scanning rate of 1.0×10^4 K/s for different time after self-nucleated at (a, b) T_s = 410 K, (c, d) T_s = 370 K, (e) T_s = 358 K, (f) T_s = 360 K

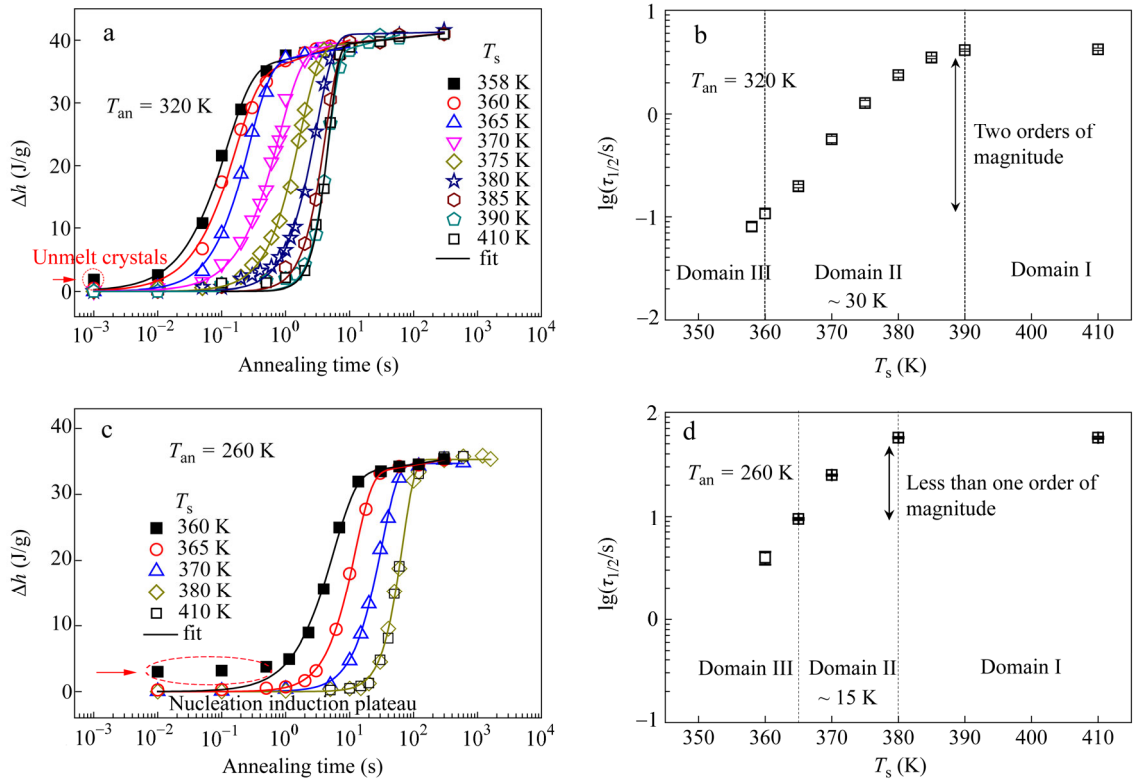

Fig. 6 Total latent heat of PBS (after treated at indicated T_s) as a function of annealing time at (a) T_{an} = 320 K and (c) T_{an} = 260 K (Each point represents a single measurement after SN at that annealing temperature.); The crystallization half-time for each curve (calculated by fitting the curve with Avrami equation) as a function of self-nucleation temperature T_s when annealing at (b) T_{an} = 320 K and (d) T_{an} = 260 K

In the current work, we suggest a characterization method of isothermal crystallization rates measured with DFSC to analyze the effect of self-nucleation. The ultra-fast cooling ability of DFSC allows an observation of crystal nucleation and growth on time scales starting from 1 ms and makes it accessible to study the effect of self-nucleation on isothermal crystallization in the whole range of temperatures where semi-crystalline polymers crystallize. As shown in Fig. 7, the crystallization half-time can be obtained for the original and self-nucleated PBS samples isothermally crystallized at different temperatures. The "ideal" T_s means the temperature at the lower limit of domain II, where the maximum number of self-nuclei may be afforded in the sample. For

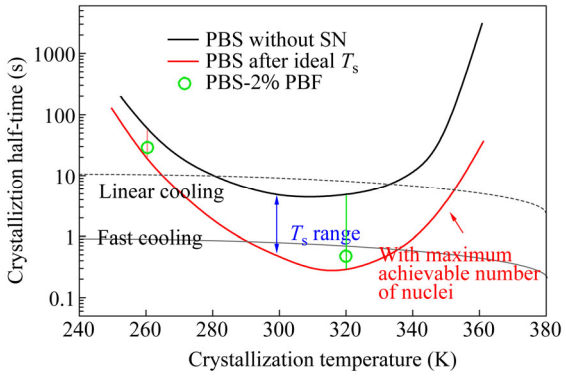

Fig. 7 Schematic representation of isothermal crystallization kinetics of original (black) and ideally self-nucleated (red) PBS sample (The dash lines show linear cooling from the melt at different rates.)

non-isothermal experiments with linear cooling performed with DSC, as schematically shown in Fig. 7 (dash line), self-nucleation makes the cross moving to higher crystallization temperature, which means a shift of crystallization peak to higher temperature in the cooling curves (as shown in Fig. 2a). This is also useful for tuning the crystallization temperature of polymers in fast cooling process. But one important thing to note is that the effective self-nucleation domain depends on the "standard" state. It is not comparable for the self-nucleation temperature region obtained from DSC and DFSC, as they have different initiate structure of crystals. And the crystallization half-time of ideally self-nucleated PBS sample (Fig. 7) may vary if the standard history is changed.

Self-nucleation experiments have also been used to judge the efficiency of nucleating agents in polymers. Control of the spherulite size by addition of nucleation agents is a facile means to modify and adapt the physical properties of bulk crystalline polymers for specific uses[37, 38]. Schneider *et al*. established an "efficiency scale" for nucleation additives of PVDF by investigating the self-nucleation phenomenon, helping rate the nucleation induced by crystalline additives[3]. The percentage of efficiency can be defined by the following Eq. (1):

$$\text{Efficiency}\ (\%) = \Delta T_c / \Delta T_{c\,max} = (T_{c\,nucl} - T_{c1})/(T_{c2} - T_{c1}) \tag{1}$$

where T_{c1} and T_{c2} are the lower and upper limits of T_c investigated in SN procedure, $T_{c\,nucl}$ is the crystallization temperature of the sample added with nucleating agents, $\Delta T_c = T_{c\,nucl} - T_{c1}$ is the increase in T_c induced by the nucleating additive, and $\Delta T_{c\,max} = T_{c2} - T_{c1}$ is the maximum range of T_c.

As discussed above, judging the nucleation efficiency by comparing the crystallization peak temperature on cooling from the melt in DSC traces is not as accurate as by the quantitative analysis under isothermal conditions with DFSC. Müller *et al*. carried out a study on the influence of multiwall carbon nanotubes (MWCNT) on nucleation of poly(ε-caprolactone) (PCL) with DSC, and found a saturation of the nucleating effect at about 0.5 wt% MWCNT concentration[22]. However, with designed experiments performed with DFSC, Zhuravlev *et al*. claimed that nucleation by MWCNTs was not yet saturated with up to 2 wt% MWCNT in PCL[23].

In analogy, Eq. (2) can be introduced to judge the efficiency of nucleating agents with crystallization half-time $\tau_{1/2}$ obtained from DFSC measurements:

$$\text{Efficiency}_{T_{an}}(\%) = \Delta\tau_{1/2}/\Delta\tau_{1/2\ max} = \left(\tau_{1/2\ nucl} - \tau_{\frac{1}{2}1}\right) \Big/ \left(\tau_{\frac{1}{2}2} - \tau_{\frac{1}{2}1}\right) \tag{2}$$

where $\Delta\tau_{1/2\ max}$ is the maximum range of $\tau_{1/2}$ for the self-nucleation procedure at a selected T_{an}, $\Delta\tau_{1/2}$ is the increase in $\tau_{1/2}$ induced by the nucleating agents at the same isothermal crystallization temperature. As the obtained crystallization half-time is of the sample crystallized at a given temperature (*e.g.* T_{an} = 320 K), the efficiency of nucleating agents calculated from this equation is only valid for the indicated crystallization temperature.

Taking PBS with 2 wt% PBF[39] as an example, we can calculate the nucleating efficiency of PBF from T_c and $\tau_{1/2}$ (Fig. 2a and Fig. 6b). It is 88% for non-isothermal crystallization and 89% for isothermal crystallization at T_{an} = 320 K, respectively. As the self-nucleation behavior depends on the initiate crystal structure of the standard sample, the efficiencies of nucleating agents calculated from these two equations are not comparable. But Eq. (2) enables a chance to calculate the approximate nucleation efficiency of additives at any selected crystallization temperature under isothermal conditions.

CONCLUSIONS

In this work, self-nucleation of PBS sample was investigated with DSC and DFSC. Instead of crystallization peak temperature T_c, the change of crystallization half-time was introduced to describe the self-nucleation behavior. And with the advantage of fast scanning rates, the effect of self-nucleation on the kinetics of isothermal crystallization was examined over a wide temperature range where PBS crystalizes. The effective self-nucleation domain varied with the annealing temperature, and homogeneous nucleation might compete with

the self-nuclei and overturn the self-nucleation effect at high supercooling. Because of the limitation of cooling abilities of conventional DSC, it was of more accuracy to judge the efficiency of nucleating agents by the change of crystallization half-time, and an equation established from self-nucleation measurements enabled the calculation of nucleation efficiency at any indicated crystallization temperature under isothermal conditions.

ACKNOWLEDGMENTS The authors gratefully appreciate the sample offered from Jun Xu and helpful discussion in related work.

REFERENCES

1 Xu, J.J., Ma, Y., Hu, W.B., Rehahn, M. and Reiter, G., Nat. Mater., 2009, 8(4): 348
2 Fillon, B., Wittmann, J.C., Lotz, B. and Thierry, A., J. Polym. Sci., Part B: Polym. Phys., 1993, 31(10): 1383
3 Schneider, S., Drujon, X., Lotz, B. and Wittmann, J.C., Polymer, 2001, 42(21): 8787
4 Supaphol, P. and Lin, J.S., Polymer, 2001, 42(23): 9617
5 Wang, K.F., Mai, K.C., Han, Z.W. and Zeng, H.M., J. Appl. Polym. Sci., 2001, 81(1): 78
6 Müller, A.J., Albuerne, J., Marquez, L., Raquez, J.M., Degée, P., Dubois, P., Hobbs, J. and Hamley, I.W., Faraday Discuss., 2005, 128: 231
7 Song, J., Chen, Q., Ren, M., Sun, X., Zhang, H., Zhang, H. and Mo, Z., J. Polym. Sci., Part B: Polym. Phys., 2005, 43(22): 3222
8 Lorenzo, A.T., Arnal, M.L., Sanchez, J.J. and Muller, A.J., J. Polym. Sci., Part B: Polym. Phys., 2006, 44(12): 1738
9 Qian, J.S., Guerin, G., Lu, Y.J., Cambridge, G., Manners, I. and Winnik, M.A., Angew. Chem. Int. Ed., 2011, 50(7): 1622
10 Yang, H., Caydamli, Y., Fang, X.M. and Tonelli, A.E., Macromol. Mater. Eng., 2015, 300(4): 403
11 Li, X.Y., Ma, Z., Su, F.M., Tian, N., Ji, Y.X., Lu, J., Wang, Z. and Li, L.B., Chinese J. Polym. Sci., 2014, 32(9): 1224
12 Mamun, A., Chen, X.J. and Alamo, R.G., Macromolecules, 2014, 47(22): 7958
13 Papageorgiou, D.G., Zhuravlev, E., Papageorgiou, G.Z., Bikiaris, D., Chrissafis, K. and Schick, C., Polymer, 2014, 55(26): 6725
14 Chen, X., Mamun, A. and Alamo, R.G., Macromol. Chem. Phys., 2015, 216(11): 1220
15 Kang, J., Peng, H.M., Wang, B., Chen, J.Y., Yang, F., Cao, Y., Li, H.L. and Xiang, M., J. Macromol. Sci. B, 2015, 54(2): 127
16 Hu, D.D., Ye, S.B., Yu, F. and Feng, J.C., Chinese J. Polym. Sci., 2016, 34(3): 344
17 Reid, B.O., Vadlamudi, M., Mamun, A., Janani, H., Gao, H.H., Hu, W.B. and Alamo, R.G., Macromolecules, 2013, 46(16): 6485
18 Wang, Y.T., Lu, Y., Zhao, J.Y., Jiang, Z.Y. and Men, Y.F., Macromolecules, 2014, 47(24): 8653
19 Wang, Y.T., Liu, P.R., Lu, Y. and Men, Y.F., Chinese J. Polym. Sci., 2016, 34(8): 1014
20 Zhao, J.Y., Sun, Y.Y. and Men, Y.F., Ind. Eng. Chem. Res., 2017, 56: 198
21 Fillon, B., Thierry, A., Lotz, B. and Wittmann, J.C., J. Therm. Anal., 1994, 42(4): 721
22 Trujillo, M., Arnal, M.L., Muller, A.J., Mujica, M.A., de Navarro, C.U., Ruelle, B. and Dubois, P., Polymer, 2012, 53(3): 832
23 Zhuravlev, E., Wurm, A., Poetschke, P., Androsch, R., Schmelzer, J.W.P. and Schick, C., Eur. Polym. J., 2014, 52: 1
24 Minakov, A.A., Mordvintsev, D.A. and Schick, C., Polymer, 2004, 45(11): 3755
25 Mileva, D., Androsch, R., Zhuravlev, E. and Schick, C., Thermochim. Acta, 2009, 492(1-2): 67
26 Kolesov, I., Mileva, D., Androsch, R. and Schick, C., Polymer, 2011, 52(22): 5156
27 Chen, L.L., Jiang, J., Zhuravlev, E., Wei, L., Schick, C., Xue, G. and Zhou, D.S., Macromol. Chem. Phys., 2015, 216(22): 2211
28 Zhuravlev, E., Schmelzer, J.W.P., Wunderlich, B. and Schick, C., Polymer, 2011, 52(9): 1983

29 Zhuravlev, E., Schmelzer, J.W.P., Abyzov, A.S., Fokin, V.M., Androsch, R. and Schick, C., Cryst. Growth Des., 2015, 15(2): 786
30 Martino, L., Guigo, N., van Berkel, J.G., Kolstad, J.J. and Sbirrazzuoli, N., Macromol. Mater. Eng., 2016, 301(5): 586
31 Ye, H.M., Tang, Y.R., Xu, J. and Guo, B.H., Ind. Eng. Chem. Res., 2013, 52(31): 10682
32 Xu, J., Heck, B., Ye, H.M., Jiang, J., Tang, Y.R., Liu, J., Guo, B.H., Reiter, R., Zhou, D.S. and Reiter, G., Macromolecules, 2016, 49(6): 2206
33 Zhuravlev, E. and Schick, C., Thermochim. Acta, 2010, 505(1-2): 1
34 Zhuravlev, E. and Schick, C., Thermochim. Acta, 2010, 505(1-2): 14
35 Xu, Y.M., Wang, Y.M., Xu, T., Zhang, J.J., Liu, C.T. and Shen, C.Y., Polym. Test., 2014, 37: 179
36 Chen, X.J., Mamun, A. and Alamo, R.G., Macromol. Chem. Phys., 2015, 216(11): 1220
37 Thierry, A., Straupe, C., Lotz, B. and Wittmann, J.C., Polym. Commun., 1990, 31(8): 299
38 Yin, H.Y., Wei, X.F., Bao, R.Y., Dong, Q.X., Liu, Z.Y., Yang, W., Xie, B.H. and Yang, M.B., CrystEngComm, 2015, 17(11): 2310
39 Ye, H.M., Wang, R.D., Liu, J., Xu, J. and Guo, B.H., Macromolecules, 2012, 45(14): 5667